JOURNAL OF MAGNETIC RESONANCE 69, 243–257 (1986)

High-Resolution Studies of Deuterium by Time-Domain Zero-Field NQR

J. M. MILLAR,* A. M. THAYER, H. ZIMMERMANN,† AND A. PINES

Department of Chemistry, University of California, Berkeley, and Materials and Molecular Research Division, Lawrence Berkeley Laboratory, Berkeley, California 94720

Received February 11, 1986; revised April 8, 1986

Time-domain zero-field NQR methods are used to determine quadrupole coupling constants and asymmetry parameters for a variety of polycrystalline solids. Results for aliphatic and aromatic groups are reported. Several cases are presented in which sites with small differences in quadrupole coupling constants are resolved, and very small (≤ 0.1) asymmetry parameters are measured. Structure in the zero-field spectrum of diethylterephthalate due to dipolar couplings between inequivalent methylene deuterons is discussed; computer simulations of the experimental spectrum yield a reasonable assignment of the electric field gradient tensor orientations without the use of single crystals.

INTRODUCTION

The nuclear quadrupole resonance parameters of a deuteron reflect the electronic environment at its site. As a result, quadrupole coupling constants are a sensitive measure of motion, structure, and bonding in solids. With the development of solid-state high-field NMR techniques, deuterium powder patterns have been studied extensively in an attempt to model systems of interest (*1*). Obtaining these spectra is often difficult as a spectrometer with high power, rapid digitization, and quick recovery capabilities is required to characterize the free induction decay of broad-line spectra (*2, 3*). In addition, these broad lineshapes are not sensitive to subtle motions, small asymmetry parameters or slight differences in quadrupolar coupling constants. Double-resonance NQR (*4, 5*) also provides a means of determining values of the quadrupole parameters but is often limited by the radiofrequency absorption of the proton system at low frequencies. Single-crystal studies (*6*) can be conducted to obtain quadrupolar information but are often tedious and time-consuming procedures which require extensive data collection and manipulation and the use of single crystals.

Zero-field deuterium NQR (*7–10*) with pulsed field cycling provides an alternative means of obtaining high-resolution quadrupolar spectra in polycrystalline solids since it removes the orientational anisotropy which produces the broad high-field lineshapes. By using either the sudden transition (*7*) or the selective indirect detection (*8*) zero-field experiments, small quadrupole coupling constants and asymmetry parameters can be determined directly from the observed frequencies. Furthermore, two-dimen-

* Current address: Department of Chemistry, Yale University, New Haven, Conn. 06511.
† Current address: Max Planck Institut fur Medizinische Forschung, Heidelberg, West Germany.

0022-2364/86 $3.00

sional versions of the time-domain zero-field experiment can yield information on frequency connectivities (*11*). In this paper we present the results of zero-field experiments on several deuterated polycrystalline organic solids and inorganic hydrates.

ZERO-FIELD NQR SPECTRUM

The sudden-transition zero-field NQR experiment (*7, 9*) and the zero-field indirect detection method (ZFID) (*8*) have been discussed previously. Calculation of the expected zero-field quadrupolar frequencies has also been treated before (*7, 9*) and we present here only a brief summary. Each quadrupolar site may be described by a quadrupolar coupling constant, e^2qQ/h, and an asymmetry parameter, η, which describes the deviation of the electric field gradient (EFG) tensor from axial symmetry. For a nonzero value of η, lines of equal intensity are expected at

$$\nu_+ = (3 + \eta)\nu_Q$$

$$\nu_- = (3 - \eta)\nu_Q$$

and

$$\nu_0 = 2\eta\nu_Q = \nu_+ - \nu_-$$

where for $I = 1$, $\nu_Q = e^2qQ/4h$. In the limit of $\eta = 0$, the spectrum collapses to lines at $3/4(e^2qQ/h)$ and zero frequency. From these spectral frequencies the values of e^2qQ/h and η may be calculated. Unfortunately, the indirect-detection experiment produces intensities distorted by the level crossing, typically producing ν_0 lines of decreased intensity and altering the relative intensities of the ν_- and ν_+ lines.

Internal molecular motions can influence the quadrupole frequencies. In the fast motion limit, i.e.,

$$\frac{1}{\tau_c} \gg \nu_{Qi}$$

for all i, where τ_c is the correlation time of the motion and ν_{Qi}, a quadrupolar frequency of the static system, the motional effect is easily calculated (*12*). In other cases motional effects can be calculated with a stochastic Liouville method (*13, 14*), similar to that applied elsewhere to the motion of coupled spins $\frac{1}{2}$ in zero field (*15*).

The assignment of the spectra is relatively straightforward if all three lines corresponding to a single deuteron are resolved. In all cases the low-frequency ν_0 lines are the most difficult to detect since receiver drift can produce artifacts in this region. Assignments to specific chemical sites is a much more difficult task but is aided by the crystal structure symmetry, which determines the number of crystallographically inequivalent sites, and by the chemical environment, which can effect the quadrupole coupling constant and asymmetry parameter.

EXPERIMENTAL

All zero-field spectra were obtained at room temperature on a 180 MHz (^{1}H) home-built spectrometer modified for the field-cycling experiment (*16*). Specific field-cycling experiments have been described in detail elsewhere (*7–9*) and the principal ones used in this work are shown in Fig. 1. Deuteration levels were estimated from solution-

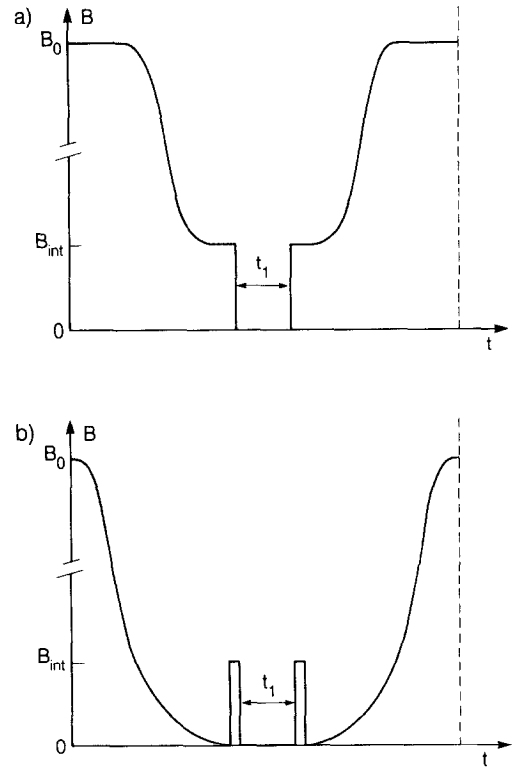

FIG. 1. Schematics of experimental field cycles. (a) Sudden-transition field cycle in which the sample is polarized in a large magnetic field, B_0, then demagnetized to an intermediate field of a few 100 G. Sudden transitions to zero field will initiate evolution for the time period t_1. Reapplication of the field terminates the zero-field period. The magnetization is measured as a function of incremented values of t_1 in successive field cycles to produce the zero-field interferogram. (b) ZFID field cycle in which demagnetization to zero field provides for level crossings in heteronuclear spin systems. The zero-field period, t_1, is initiated and terminated by pulse dc fields of 100–400 G applied for 1–2 μs. The deuteron system alone can be caused to evolve by setting the dc pulses to $\theta = \gamma_H B_i \tau = 2\pi$ for the protons. After remagnetization, the magnetization is measured in high field and the field cycle is repeated as in (a).

state NMR measurements, mass spectroscopy data, and, in the simplest cases such as the hydrates, from the manner of preparation and recrystallization. Perdeuterated samples were measured directly using the sudden transition version of the field cycle (*7, 9*) (Fig. 1a), with an intermediate field of ~300 G. After demagnetization to the intermediate field, the sudden switch off of the field will initiate zero-field evolution. The evolution period, t_1, is terminated by reapplication of the field and followed by remagnetization. Sampling of the magnetization in high field for incremented values of t_1 produces the zero-field interferogram. Repetition rates depend upon the T_1 of the specific compound studied but, on average, collection of approximately 1000 data points takes several hours.

Specifically labeled or partially deuterated compounds were observed indirectly (*8*) via ^2H–^1H level crossings which occur as a consequence of the demagnetization and

remagnetization field cycle shown in Fig. 1b. Indirect detection of the deuteron NQR spectrum through the high γ protons should lead to an increase in sensitivity. The pulsed dc fields of ~100–300 G initiate and terminate the zero-field t_1 period in a manner analogous to that of the sudden field transitions of the previous field cycle. Selective observation of only the ^{2}H zero-field evolution is possible by calibrating the dc pulses to correspond to 360° pulse angles for the protons (*8*). Experimental times were determined primarily by the T_1 of the compound of interest, and advantageous proton relaxation times were often found in the indirect detection experiments.

RESULTS AND DISCUSSION

Deuterium quadrupole coupling constants have been studied extensively by a variety of techniques and are reviewed in the literature (*5, 17–19*). The present work is an extension of these results providing determination of low-frequency ν_0 transitions, resolution of individual ring sites, and measurement of small asymmetry parameters. The deuterium quadrupole coupling constants and asymmetry parameters for a variety of compounds are reported in Table 1. Spectra produced by the sudden transition field cycle are marked by an asterisk in the table. Errors in reported values depend upon distinct features of each spectrum such as linewidth, resolution, and signal-to-noise but can be as low as ±0.1 kHz for the e^2qQ/h values and ±0.001 for the asymmetry parameters. Overall the asymmetry parameters are found to be small, <0.1, and as such would be difficult or impossible to measure from high-field powder patterns. As will be illustrated in detail later, the presence of two or more very similar deuteron sites with slightly different e^2qQ/h and η values which could not be distinguished by high-field powder measurements are often resolved in zero field.

Aromatic Carboxylic Acids and Esters

In this section, we present data regarding the quadrupole coupling constants and asymmetry parameters of different aromatic sites. Deuterium quadrupolar coupling constants have been reported for aromatic sites in a variety of systems (*17, 18, 20, 21*) and cover a range of ~165–195 kHz although the asymmetry parameter is often undetermined. Often only the average quadrupole coupling constant over all sites on the ring is reported. In contrast, our data in Table 1 shows that ring substituents can alter the environment of the aromatic deuterons, producing splittings that are resolvable in the zero-field spectrum.

Terephthalic acid. The simplest case presented is that of terephthalic acid as seen in Fig. 2. The spectrum consists of four relatively broad (~1.5 kHz) lines at 3.0, 11.1, 131.4, and 134.3 kHz. The inverted feature at 11.1 kHz is most probably attributable to the proton dipolar signal of the motionally averaged carboxylic acid dimers (*22, 23*). The COOH group is ~60% deuterated but due to the large distances in the dimer the efficiency of the level crossing is such that no ^{2}H signal is observed. The three remaining lines form the $\nu_0/\nu_-/\nu_+$ triplet which results in the value in Table 1. The observed linewidths (~1.5 kHz) are considerably greater than those observed in the ZFID spectra of the aromatic sites of toluic acid and benzoic acid, which are both ~0.8 kHz. This increased linewidth and the asymmetric appearance of the terephthalic

TABLE 1

Deuterium Quadrupole Coupling Constants and Asymmetry Parameters

		This work		Literature[a]	
		e^2qQ/h	η	e^2qQ/h	η[c]
Aromatic carboxylic acids and esters					
Diethyl terephthalate (CD_2)*		149.63	0.041		
		152.67	0.049		
Diethyl terephthalate (ring)*		180.53	0.022		
		178.33	0.015		
Terephthalic acid		177.3	0.033		
Toluic acid		173.74	0.028		
		178.92	0.023		
Benzoic acid[b]	*ortho*	177.80	0.040		
	meta	179.70	0.026		
	para	172.95	0.010		
Alkanes					
Nonadecane 2,2-d_2		74.03	0.39	72.7[31]	0.36
Polyethylene $(-CD_2-)_n$*		164.93	<0.01	163.9[29]	NR
Carboxylic acid salts and amines					
α-Glycine (CD_2)*		160.09	0.042	159.99[6]	0.043
		169.01	0.092	169.41[6]	0.085
Na propionate (CD_2)		170.14	<0.02		
Hydrates and metal sandwich compounds					
$Li_2SO_4 \cdot HDO$		123.05	0.81	123 ± 3[38-9]	0.80 ± 0.02
$Ba(ClO_3)_2 \cdot HDO$		122.7[40]	0.96	121.5 ± 0.4[34]	0.976 ± 0.007
Ferrocene-d_{10}*		193.8	<0.01	198 ± 2[21]	NR

[a] Error limits where quoted are those of the respective author(s), superscripts indicate reference numbers.

[b] *Ortho, meta,* and *para* assignments made as discussed in text.

[c] References for asymmetry parameters, when reported, are the same as those of the corresponding e^2qQ/h value.

* Denotes spectra obtained with sudden transition field cycle on perdeuterated compounds, all others were indirectly detected (ZFID).

acid aromatic lines certainly suggests the unresolved structure of similar sites. This is in line with X-ray data (*24*) which predicts two crystallographically inequivalent sites.

Toluic and benzoic acids. The spectra of toluic and benzoic acids are similar to that of terephthalic acid. In the former case two sites are resolved, those *ortho* to the COOH and those meta to the COOH. Benzoic acid produces a more complicated spectrum with at least six high-frequency lines. If we assume three resolvable sites, then the only consistent assignment of e^2qQ/h and η values is that given in Table 1. We can further assign these quadrupole parameters to specific sites of the ring with the following qualitative arguments. First, we expect the electronegative oxygens, due to their proximity, to increase the asymmetry parameters of the deuterons sites resulting in

$$\eta_{ortho} > \eta_{meta} > \eta_{para}.$$

Second, it has been shown (*17*) that electron donating groups, such as $-NH_2$, increase the average quadrupole coupling constant relative to that observed in the unsubstituted benzene. By the same argument, one expects an electron withdrawing group, such as $-COOH$, to decrease the average quadrupole coupling constant of the ring. From the resonance arguments of basic organic chemistry (*25*) one expects the electron withdrawing effect to be greatest at the *ortho* and *para* sites. With these arguments we make the site assignments of Table 1.

Diethyl terephthalate. We have performed extensive studies on diethyl terephthalate both in high field and zero field in an effort to compare the information available from the two methods. From the high-field NMR spectrum, three broad overlapping powder patterns corresponding to methyl, methylene, and aromatic sites are resolved. The well resolved zero-field spectrum provides a good example of the resolution of several quadrupolar sites and the effect of dipolar coupling on NQR spectra and we will treat this matter in detail.

The zero-field deuterium NQR spectrum of perdeuterated polycrystalline diethyl-terephthalate appears in Fig. 3. As this spectrum was observed directly using the sudden transition field cycle, the intensities reflect the individual deuteron signals. Four distinct regions (also shown expanded in Fig. 4) are observed corresponding to the low-frequency ν_0 lines, methyl, methylene, and aromatic sites, in increasing order of frequency. The symmetric shape of the methyl region corresponds to that obtained in simulations of methyl groups whose motionally averaged asymmetry parameters were equal to zero (*9*). From this we expect no methyl group contribution to the ν_0 region. The

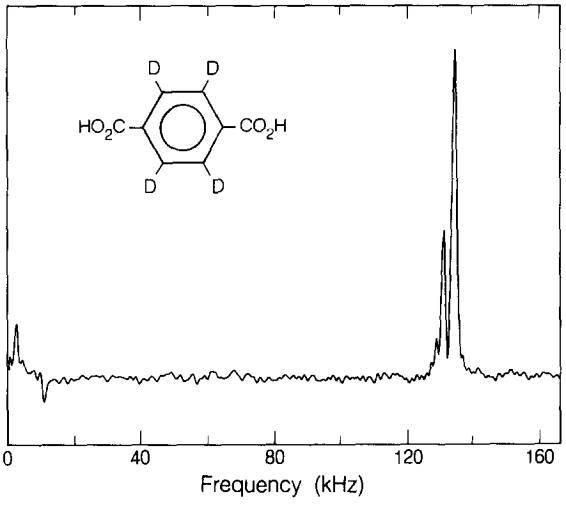

FIG. 2. ZFID spectrum of terephthalic acid (98% d_4, 60%COOD). Three of the four lines are assigned to the single resolved site and the fourth at 11.1 kHz is assigned to the proton signal of the carboxylic acid dimers (*22, 23*). We conclude that no signal is contributed from the carboxylic acid deuterons due to the absence of their ν_+ and ν_- lines which are expected at 135.5 and 119.5 kHz on the basis of previous work on benzoic acid (*37*).

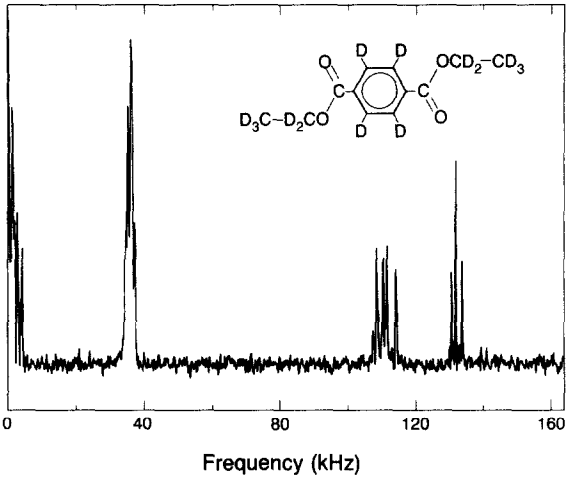

FIG. 3. Sudden-transition zero-field ^{2}H NQR spectrum of perdeuterated diethylterephthalate. Four regions are clearly evident; from right to left the three line aromatic region, the methylene region, the methyl region, and the ν_0 region. In contrast to the powder spectrum, the signal from an individual site is no longer distributed over the entire broad frequency bandwidth. Instead, many narrow (~300 Hz) lines are resolved corresponding to deuteron sites with small differences in quadrupolar coupling constants and asymmetry parameters.

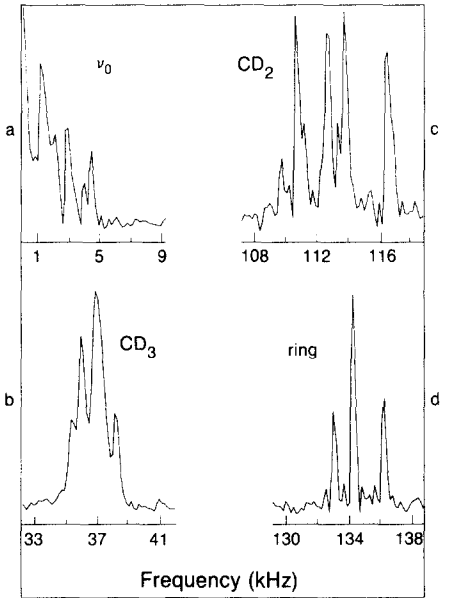

FIG. 4. Expanded plots of the individual regions of the sudden-transition zero-field NQR spectrum of perdeuterated diethylterephthalate. The methyl group lineshape, indicative of an $\eta = 0$ site, produces no contributions to the ν_0 region. Since $\eta \neq 0$ for an aromatic site, the central line in (d) must consist of the superposition of the ν_+ and ν_- lines of two different sites. This assignment can be confirmed by the ν_0 lines at 1.2 and 2.0 kHz which are observed in (a). The deuteron–deuteron dipolar coupling in the CD_2 group produces the splittings observed in the ν_+/ν_- lines of (c) as well as in the ν_0 lines seen in (a). The principal features of these regions can be used to calculate quadrupolar coupling constants for two inequivalent methylene deuterons.

aromatic region between 132 and 137 kHz shows three lines with an intensity ratio of 1:2:1. Since η is generally nonzero for an aromatic site (*1*), the observed signal can be interpreted by assuming two aromatic sites where the ν_+ of one site and the ν_- of the other overlap to form the central line. The low-frequency lines observed at 1.2 and 2.1 kHz support this conclusion although from Fig. 4 one sees they are just at the limits of experimental resolution.

The methylene region of diethylterephthalate contains four major lines and additionally shoulders and smaller satellite lines. The major lines are lower in frequency by 40–400 Hz from the lines found in the previously reported zero-field indirect detection spectrum (*8*). The ν_0 region contains two features whose frequencies coincide with those predicted from the ZFID measurement; however, the feature at higher frequency shows a well resolved splitting. Calculation of the quadrupolar parameters directly from this sudden spectrum yields $(e^2qQ/h)_1 = 149.63 \pm 0.1$ kHz, $\eta_1 = 0.041 \pm 0.001$, $(e^2qQ/h)_2 = 152.67 \pm 0.1$ kHz, and $\eta_2 = 0.049 \pm 0.001$, which are all within the experimental error of the earlier measurement. These values correspond to the two deuterons of an individual methylene group which are inequivalent based on crystallographic effects (*26*).

The deviation of the observed CD_2 spectrum from the simple six-line spectrum expected for two uncoupled deuterons is a consequence of the dipolar interaction between the two methylene deuterons. Similar effects have been observed in other materials using frequency-domain double-resonance NQR techniques (*27*). The details of the interaction are complicated since the dipolar perturbed spectrum depends on at least ten variables (*28*). These are $r_{D\text{-}D}$, the deuteron–deuteron internuclear distance; the quadrupole coupling constants and asymmetry parameters of both deuterons; the Euler angles α, β, γ which relate the electric field gradient tensor of deuteron one to deuteron two; and finally θ, ϕ, the spherical polar coordinates of $r_{D\text{-}D}$ in the principal axis system of deuteron one. With reasonable estimates of some of the parameters we can hope to get at least an idea of the orientation of the electric field gradient tensors in the molecular frame.

The simulations used the quadrupolar parameters of Table 1 (which were calculated directly from the sudden transition spectrum) and we assumed the principal z axes of the EFG tensors lay along the respective C–D bonds (*6c*). We also assumed a geometry with $r_{D\text{-}D} = 1.81$ Å and a D–C–D bond angle of 109.5°. Two sets of simulations were performed; these differed in that the first assumed that the two quadrupolar tensors are related by a C_2 rotation about the D–C–D bisector and the second assumed that the tensors were related by a rotation of 109.5° about an axis passing through the carbon atom and perpendicular to the D–C–D plane. We informally refer to these as the flip and kick models, respectively. This seems like a reasonable starting point since single-crystal measurements have found comparable situations in glycine (*6c*) and malonic acid (*6d*). A similar approximation was used in the analysis of double-resonance studies by Edmonds *et al.* (*27*). A full set of simulations encompassing all possible orientations was beyond the scope of the present work. Typical examples of the simulations are shown in Fig. 5. The geometry which produced the best agreement is that shown in Fig. 6 where the tensors are in a "flip" configuration and each tensor has its x principal axis oriented $\sim 10°$ out of the D–C–D plane. The major features of the experimental spectra are reproduced by the simulation.

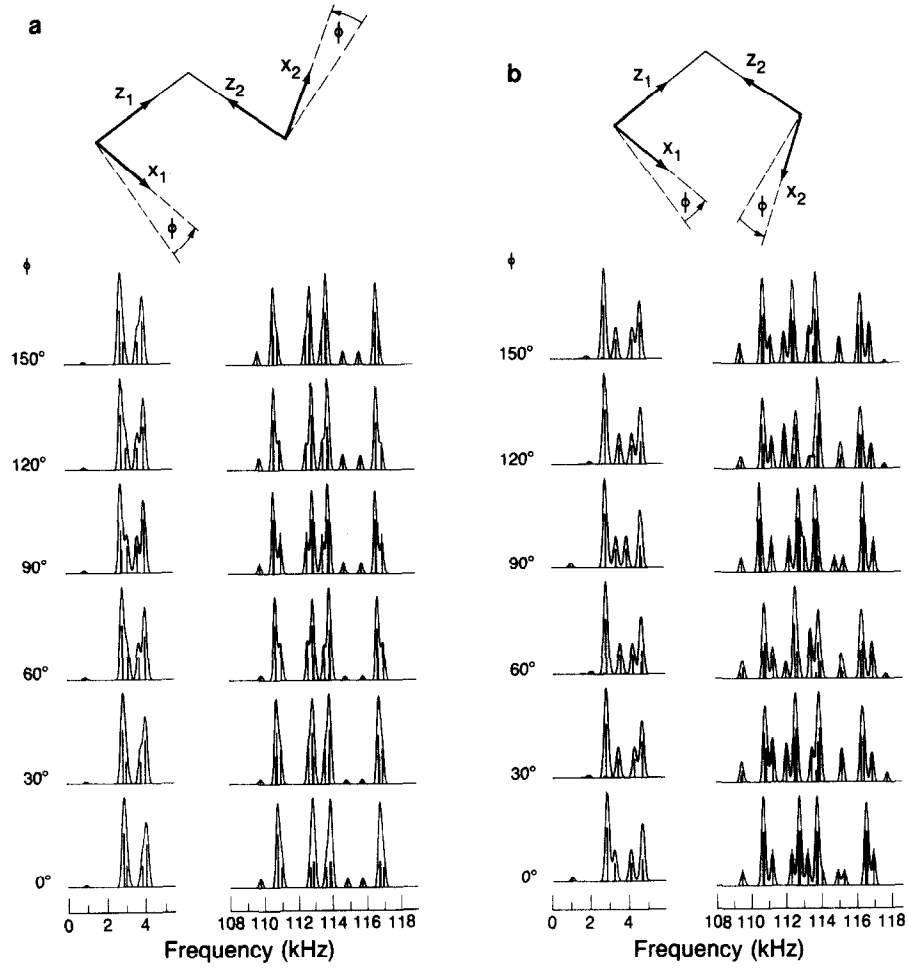

FIG. 5. Computer simulations of the ν_0 and high-frequency lines of two dipolar coupled deuterons. Both sets assume an internuclear distance of 1.81 Å and a tetrahedral bond angle (109.5°). The z axes of the EFG tensors are taken to be along the C–D bonds. Quadrupole coupling constants used are those reported in Table 1 calculated from the principal lines in the spectrum. The parameter varied in the simulations corresponds to the relative orientation of the dipolar axis in the EFG tensor frame. As shown in (a), the two tensors are related by a rotation of 109.5° about an axis perpendicular to the DCD plane and passing through the carbon atom. The dipolar coupling produces a relatively small perturbation in the six-line spectrum with satellite lines low in intensity and the shoulders less well resolved. In the second set (b), the EFG tensors are related by a 180° rotation about the DCD bisector. In this case the spectral frequencies and lineshapes are more sensitive to the variations in ϕ. The satellite lines and shoulders are more prominent.

Alkanes and Long Chain Carboxylic Acids

Polyethylene. Polyethylene has been the subject of considerable study by high-field NMR (*1, 29*) and Fig. 7 shows the sudden-transition zero-field spectrum from which one calculates $e^2qQ/h = 164.9$ and $\eta \leq 0.01$ reflecting the relatively restricted motion of the chains and in good agreement with the literature values obtained from powders

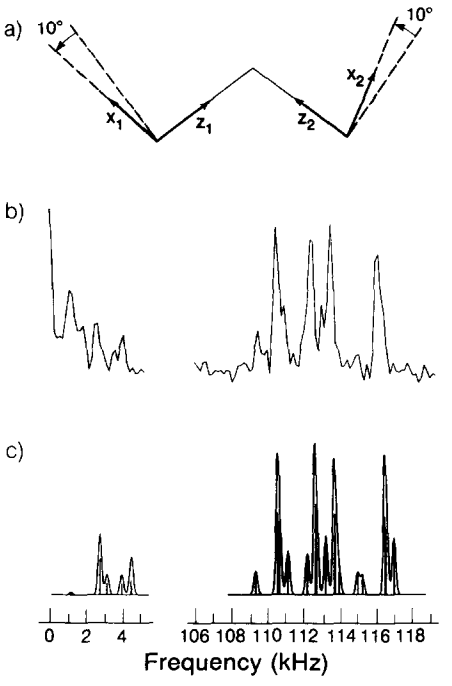

FIG. 6. Results of simulations for CD_2 in diethyl terephthalate. (a) EFG tensor orientation producing best fit of the experimental spectrum. Tensor 1 (left), is related to tensor 2 by a 180° flip about the C_2 axis. The x_1 axis lies ~10° below the DCD plane and x_2 lies ~10° above. (b) Reproduction of the ν_0 region and methylene ν_+/ν_- region (note that the experimental ν_0 region contains a split line at ~1 kHz due to the aromatic deuterons). (c) Best-fit simulation of the CD_2 deuterons. Parameters are given in text and a gaussian broadening function was applied to simulate the linewidth.

(*29*). Only the crystalline region of the material contributes to the spectrum since the short T_1 of the amorphous region (*30*) prevents its survival in the experimental field cycle. The linewidth of several kilohertz is likely a reflection of a distribution of quad-

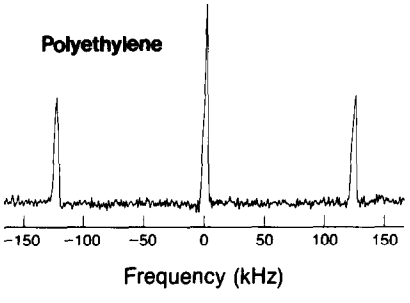

FIG. 7. Sudden-transition zero-field spectrum of ~60–80% crystalline polyethylene. Both positive and negative frequencies are plotted to show the relative intensities of the zero frequency and ±123.7 kHz lines. The integrated intensities are in the ratio 1:1.6:1 in contrast to the 1:1:1 expected for an $\eta \sim 0$ spin one nucleus. In addition, the broad, slightly asymmetric lineshape of the ±123.7 kHz lines may indicate a distribution of quadrupole coupling constants.

rupole coupling constants which is produced by a distribution of motions throughout the crystalline region.

The polyethylene spectrum shows a 1:1.6:1 ratio of peaks in contrast to the 1:1:1 ratio expected for an $\eta \simeq 0$ system in the sudden transition experiment. Computer simulations of zero-field spectra have shown (*13*) that even motions whose frequency are $\sim\frac{1}{100}$ of the quadrupolar frequencies can produce an increase in the relative intensity of the zero-frequency line; therefore the zero-field experiment should be very useful in studying slow motions in the solid state.

Nonadecane-d_2. In contrast, the torsional oscillation found in the terminal methylene group in nonadecane produces a zero-field spectrum characterized by $e^2qQ/h = 74.03$ and $\eta = 0.39$, which is close to the values reported from high-field powder measurements (*31*). Here the motion is much less restricted than in the polyethylene case, and the two together give an idea of the extremes of motion that can occur in different positions of long chains.

Lauric acid. The zero-field spectrum of highly deuterated long chain molecules may not be simple or well resolved. As an example, the zero-field NQR spectrum of polycrystalline perdeuterated lauric acid is shown in Fig. 8. Three regions appear in the spectrum and are attributable to ν_0, methyl, and methylene/carboxylic acid deuterons. Few resolved features are seen in the methylene region of the spectrum which is substantially broader in comparison to polyethylene. The lineshape may be a result of unresolved dipolar couplings but the breadth of the ν_0 and high-frequency methylene lines is most likely an indication of a distribution of quadrupolar sites and asymmetry parameters. Similarly to the polyethylene case, this distribution of quadrupole couplings may be a result of low-amplitude motions.

Hydrates

Two further examples of how rapid motion manifests itself in zero field are provided by the inorganic hydrates $Ba(ClO_3)_2 \cdot H_2O$ and $Li_2SO_4 \cdot H_2O$. In the solid state the water molecules execute rapid 180° flips about their C_2 axes (*19, 32*) in combination

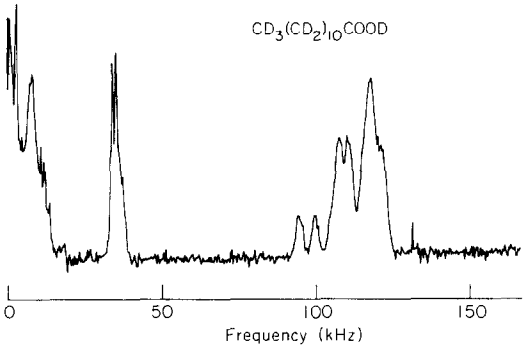

FIG. 8. Zero-field deuterium NQR spectrum of perdeuterated polycrystalline lauric acid. The ν_0, methyl, and methylene regions appear in order of increasing frequency. Due to the broad lineshapes which result from dipolar couplings and a distribution of quadrupolar couplings, no simple assignment of the quadrupolar sites can be made.

with librations about three perpendicular axes (*19, 33*). A simple calculation (*18, 34*) shows the flipping motion averages the quadrupole coupling constant to $\sim\frac{1}{2}$ the static value and in addition produces an average asymmetry parameter of $\eta \sim 1$. (Chiba (*34*) reports $e^2qQ/h = 243.5$ kHz and $\eta = 0.074$ for the static D_2O in barium chlorate.) The zero-field indirect detection NQR spectrum of lithium sulfate, Fig. 9, shows the three-line structure expected for the $\eta \neq 0$ deuterons. An additional peak of low-intensity appears at 28.0 kHz due to the spin-$\frac{3}{2}$ ^{7}Li (*7*). The intensities are distorted due to the level crossings dynamics and the calculated quadrupole coupling constant of 123.05 kHz and $\eta = 0.81$ are in good agreement with that expected from the above arguments.

Carboxylic Acid Salts and Amines

Sodium propionate. The zero-field spectrum of sodium propionate shows a line centered at ~127 kHz and one at zero frequency. A slightly asymmetric shape indicates the possibility of a non-axially symmetric electric field gradient for which one calculates $\eta \leq 0.02$. The calculated value of e^2qQ/h is close to that as expected for a C–D bond in a rigid solid (*1*).

Glycine. The sudden-transition zero-field spectrum of α-glycine (Fig. 10) indicates two methylene sites whose quadrupole coupling constants are calculated to be $(e^2qQ/h)_1 = 160.09$, $\eta_1 = 0.042$, $(e^2qQ/h)_2 = 169.01$ kHz and $\eta_2 = 0.092$. The ND_3^+ group does not contribute due to its short T_1 (~3 ms (*6c*)) and the line at zero frequency is an impurity. The quadrupole parameters obtained in single-crystal studies (*6c*), Table 1, are in substantial agreement with the above, although the differences in the corresponding values of $(e^2qQ/h)_1$ and η_1 appear to be outside the range of the experimental error of both experiments. We would expect that the zero-field measurements to be slightly more accurate since they do not have the problems and errors associated with

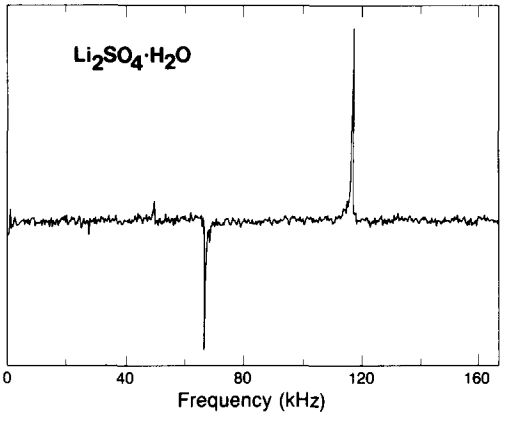

FIG. 9. ^{2}H ZFID spectrum of 50% deuterated lithium sulfate monohydrate. The ν_+, ν_-, and ν_0 lines of the motionally averaged water molecules are clearly observed at 117.19, 67.38, and 50.13 kHz. The linewidths are ~0.53 kHz. A small peak at 28.0 kHz is due to the zero-field spectrum of the spin-$\frac{3}{2}$ ^{7}Li. The intensities of the lines are a function of the level crossings in the demagnetization and remagnetization steps of the field cycle.

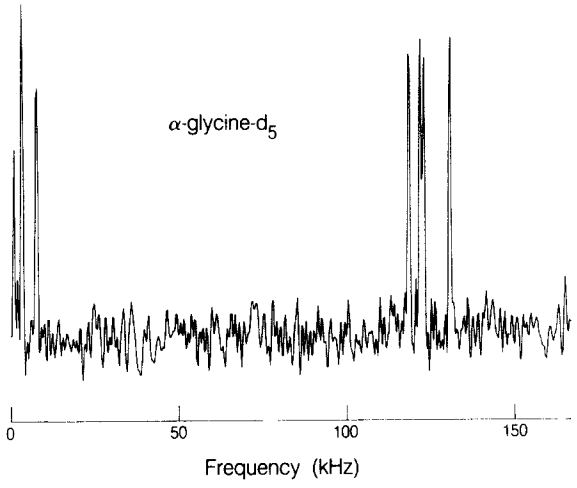

FIG. 10. Sudden-transition zero-field ^2H spectrum of α-glycine-d_5. The six lines predicted for the two methylene sites are clearly visible yielding the calculated quadrupolar parameters of Table 1. No signal is observed from the ND_3^+ due to its short T_1. An artifact appears at zero frequency.

crystal mounting and also because the zero-field linewidths of 1 kHz are only two-thirds of those reported for the single-crystal measurements.

Ferrocene

The metal sandwich compound ferrocene consists of an iron atom between two coplanar cyclopentadienyl rings which are known to undergo rapid rotation about their C_5 axes (*35, 36*). High-field measurements at 113 K obtained a value of $e^2qQ/h = 198 \pm 2$ kHz for the quadrupole coupling constant under the assumption of a zero asymmetry parameter (*21*). Our room-temperature zero-field measurements obtained the value of 193.8 ± 0.5 kHz with an asymmetry parameter $\eta \leqslant 0.01$. The large value of the quadrupole coupling constant can be attributed to the presence of the iron atom (*21*).

CONCLUSION

We have presented deuterium NQR results for a variety of compounds using two versions of the zero-field NQR experiment. Unlike high-field powder spectra, the frequencies of interest are measured directly from relatively narrow lines. The time-domain nature of the experiment and the selectivity of the pulsed dc fields allows measurement of the low-frequency ν_0 lines, while avoiding problems of power broadening and the absorption of the zero-field radiofrequency irradiation by the proton system (*5*). The high resolution obtained permits precise determination of quadrupole coupling constants and small asymmetry parameters in polycrystalline and amorphous materials. Assignment of specific sites with small differences in quadrupole coupling constants is possible. Structure in the lineshapes due to dipolar couplings provide information about the molecular frame orientations of the electric field gradient tensors

without requiring the use of single crystals. In addition, frequencies and intensities in the spectra may provide information on motional effects. Further work in this area is in progress.

ACKNOWLEDGMENTS

We thank A. Bielecki and D. B. Zax for the glycine and lauric acid spectra, and G. Davenport for the ferrocene data. This work was supported by the Director, Office of Energy Research, Office of Basic Energy Sciences, Material Sciences Division of the U.S. Department of Energy, and by the Director's Program Development Funds of the Lawrence Berkeley Laboratory under Contract DE-AC03-76SF00098.

REFERENCES

1. H. W. SPIESS, *in* "Advances in Polymer Science" (H. H. Kausch and H. G. Zachmann, Eds.), Vol. 66A, p. 23, Springer, Berlin, 1985; H. W. SPIESS, *Coll. Polym. Sci.* **261,** 261 (1983).
2. P. M. HENRICHS, J. M. HEWITT, AND M. LINDER, *J. Magn. Reson.* **60,** 280 (1984).
3. R. HENTSCHEL AND H. W. SPIESS, *J. Magn. Reson.* **35,** 157 (1979).
4. R. E. SLUSHER AND E. L. HAHN, *Phys. Rev. Lett.* **12,** 246 (1964); R. E. SLUSHER AND E. L. HAHN, *Phys. Rev.* **166,** 332 (1963); A. G. REDFIELD, *Phys. Rev.* **130,** 589 (1963).
5. D. T. EDMONDS, *Phys. Rep. C* **29,** 233 (1977); D. T. EDMONDS, *Int. Rev. Phys. Chem.* **2,** 103 (1982).
6. (*a*) D. M. ELLIS AND J. L. BJORKSTAM, *J. Chem. Phys.* **46,** 4460 (1967); (*b*) W. DERBYSHIRE, T. C. GORVIN, AND D. WARNER, *Mol. Phys.* **17,** 401 (1969); (*c*) C. MULLER, W. SCHAJOR, H. ZIMMERMANN, AND U. HAEBERLEN, *J. Magn. Reson.* **56,** 235 (1984); (*d*) C. MULLER, S. IDZIAK, N. POSLEWSKI, AND U. HAEBERLEN, *J. Magn. Reson.* **48,** 227 (1982).
7. A. BIELECKI, J. B. MURDOCH, D. P. WEITEKAMP, D. B. ZAX, K. W. ZILM, H. ZIMMERMANN, AND A. PINES, *J. Chem. Phys.* **80,** 2232 (1984).
8. J. M. MILLAR, A. M. THAYER, A. BIELECKI, D. B. ZAX, AND A. PINES, *J. Chem. Phys.* **83,** 934 (1985).
9. D. B. ZAX, A. BIELECKI, K. W. ZILM, A. PINES, AND D. P. WEITEKAMP, *J. Chem. Phys.* **83,** 4877 (1985).
10. R. KREIS, D. SUTER, AND R. R. ERNST, *Chem. Phys. Lett.* **118,** 120 (1985).
11. A. M. THAYER, J. M. MILLAR, AND A. PINES, *Chem. Phys. Letts.*, in press.
12. T. P. DAS AND E. L. HAHN, *in* "Solid State Physics" (F. Seitz and D. Turnbull, Eds.), Suppl. 1, Academic Press, New York, 1958.
13. P. MEIER, private communication.
14. M. MEHRING, P. JONSEN, AND M. LUZAR, personal communication.
15. J. W. HENNEL, A. BIRCZYNSKI, S. F. SAGNOWSKI, AND M. STACHUROWA, *Z. Phys. B. Cond. Matt.* **60,** 49 (1985).
16. A. BIELECKI, D. B. ZAX, K. W. ZILM, AND A. PINES, *Rev. Sci. Instrum.* **57,** 393 (1986).
17. M. RINNE AND J. DEPIREUX, *in* "Advances in NQR" (J. A. S. Smith, Ed.), Vol. 1, p. 357, Heyden, London, 1974.
18. R. G. BARNES, *in* "Advances in NQR" (J. A. S. Smith, Ed.), Vol. 1, p. 335, Heyden, London, 1974.
19. L. W. REEVES, *in* "Progress in NMR Spectroscopy" (J. W. Emsley, J. Feeney, and L. H. Sutcliffe, Eds.), Vol. 4, p. 193, Pergamon, Oxford, 1969.
20. J. L. RAGLE, M. MOKARRAM, D. PRESZ, AND G. MINOT, *J. Magn. Reson.* **20,** 195 (1975).
21. P. L. OLYMPIA, JR., I. Y. WEI, AND B. M. FUNG, *J. Chem. Phys.* **51,** 1610 (1969), and references therein.
22. B. H. MEIER, F. GRAF, AND R. R. ERNST, *J. Chem. Phys.* **76,** 767 (1982).
23. J. M. MILLAR, Ph.D. thesis, Department of Chemistry, University of California, Berkeley, 1986.
24. M. BAILEY AND C. J. BROWN, *Acta Crystallogr.* **22,** 387 (1967).
25. R. T. MORRISON AND R. T. BOYD, "Organic Chemistry," 3rd ed., Allyn & Bacon, Boston, 1976.
26. M. BAILEY, *Acta Crystallogr.* **2,** 120 (1949).
27. D. T. EDMONDS, M. J. HUNT, AND A. L. MACKAY, *J. Magn. Reson.* **20,** 505 (1975); D. T. EDMONDS, M. J. HUNT, AND A. L. MACKAY, *J. Magn. Reson.* **11,** 77 (1973).
28. S. VEGA, *in* "Advances in Magnetic Resonance" (J. S. Waugh, ed.), Vol. 6, p. 259, Academic Press, New York, 1973.

29. D. HENTSCHEL, H. SILLESCU, AND H. W. SPIESS, *Makromol. Chem.* **180,** 241 (1979).
30. D. HENTSCHEL, H. SILLESCU, AND H. W. SPIESS, *Macromolecules* **14,** 1607 (1981).
31. M. G. TAYLOR, E. C. KELUSKY, I. C. P. SMITH, H. L. CASAL, AND D. G. CAMERON, *J. Chem. Phys.* **78,** 5108 (1983).
32. A. J. SILVIDI, J. W. MCGRATH, AND D. F. HOLCOMB, *J. Chem. Phys.* **41,** 105 (1964).
33. A. ERIKSSON, M. A. HUSSEIN, B. BERGLUND, J. TEGENFELDT, AND J. LINDGREN, *J. Mol. Struct.* **52,** 95 (1979).
34. T. CHIBA, *J. Chem. Phys.* **39,** 947 (1963).
35. C. H. HOLM AND J. A. IBERS, *J. Chem. Phys.* **30,** 885 (1959).
36. L. N. MULAY AND A. ATTALLA, *J. Am. Chem. Soc.* **185,** 702 (1963).
37. T. L. BROWN, L. G. BROWN, D. Y. CURTIN, Y. HIYAMA, I. C. PAUL, AND R. B. WILSON, *J. Am. Chem. Soc.* **104,** 1172 (1982); I. J. F. POPLETT AND J. A. S. SMITH, *J. Chem. Soc. Faraday Trans.* **77,** 1473 (1981).
38. S. KETUDAT AND R. V. POUND, *J. Chem. Phys.* **26,** 708 (1957).
39. B. BERGLUND AND J. TEGENFELDT, *J. Mol. Struct.* **39,** 207 (1977).
40. J. M. MILLAR, A. M. THAYER, D. B. ZAX, AND A. PINES, *J. Am. Chem. Soc.*, in press.